

See discussions, stats, and author profiles for this publication at: <https://www.researchgate.net/publication/41571171>

Northern Hemisphere stratospheric summer from MIPAS observations

ARTICLE in QUARTERLY JOURNAL OF THE ROYAL METEOROLOGICAL SOCIETY · JANUARY 2007

Impact Factor: 3.25 · DOI: 10.1002/qj.24 · Source: OAI

CITATIONS

17

READS

28

3 AUTHORS, INCLUDING:



[W. A. Lahoz](#)

Norwegian Institute for Air Research

139 PUBLICATIONS **1,602** CITATIONS

[SEE PROFILE](#)



[Y.J. Orsolini](#)

Norwegian Institute for Air Research, also a...

101 PUBLICATIONS **1,605** CITATIONS

[SEE PROFILE](#)

Northern Hemisphere stratospheric summer from MIPAS observations

W. A. Lahoz,^{a*} A. J. Geer^{a†} and Y. J. Orsolini^b

^a Data Assimilation Research Centre, DARC, University of Reading, UK

^b NILU, Norway

ABSTRACT: Data from the MIPAS instrument on Envisat, supplemented by meteorological analyses from ECMWF and the Met Office, are used to study the meteorological and trace-gas evolution of the stratosphere in the Northern Hemisphere during spring and summer 2003. A Pole-centred approach, together with sequences of vertical profiles along the viewing tracks of the MIPAS instrument, is used to interpret the data in the physically meaningful context of the evolving summertime high. During April the vortex break-up and build-up of the summertime high gives rise, in the mid-stratosphere, to a ‘frozen-in’ anticyclone (FrIAC), over the Pole, encircled by vortex fragments at $\sim 50^\circ\text{N}$. As the summer moves on, the FrIACs and vortex fragments are gradually smoothed out but they persist in the mid- and upper stratosphere until July–August as roughly zonally symmetric W-shaped tracer isopleths. The persistence of the W shows the slowness of isentropic mixing processes at these levels during the summer. As the summertime high becomes dominant during June–August, net photochemical ozone loss produces a low ozone pool in the lower and mid-stratosphere. Finally, as the summertime high decays and the wintertime polar vortex builds up from September onward, the low ozone pool extends vertically throughout the stratosphere, and the tracer isopleths at high latitudes start to dip, showing the effects of wintertime diabatic descent. Of these features, to our knowledge, the W-shaped tracer isopleths have not been observed previously. Copyright © 2007 Royal Meteorological Society

KEY WORDS vortex break-up; summertime high; trace-gas transport; frozen-in anticyclones; vortex fragments; low ozone pool

Received 15 May 2006; Revised 23 August 2006

1. Introduction

The structure and evolution of the summer stratosphere in the Northern Hemisphere (NH) has been relatively little studied compared with stratospheric winter. Of the studies of the NH summer stratosphere, we can note the prediction of long-lived ‘fossil’ debris from the winter polar vortex (Orsolini, 2001), evidence for which was recently provided by *in situ* observations (Durry and Hauchecorne, 2005); the identification and study of summer low ozone episodes (LOEs) at northern high latitudes (Orsolini *et al.*, 2003); and the recent discovery of a ‘frozen-in’ anticyclone (FrIAC) in the spring and summer stratosphere of 2005 (Manney *et al.*, 2006). The dynamics and chemistry of springtime vortex remnants in the Arctic have been studied by Konopka *et al.* (2003). The dynamics and chemistry of the summer stratosphere have been discussed, respectively, by Wagner and Bowman (2000) and Fahey and Ravishankara (1999).

Understanding the structure and evolution of the summer stratosphere has been hampered by the relative scarcity of height-resolved global satellite observations. For example, for ozone, previous satellite observations

were limited to narrow latitude bands, because they used solar occultation (Park and Russell, 1994; Luo *et al.*, 1997; Hoppel *et al.*, 1999), were limited in time (Froidevaux *et al.*, 1994), or the only global measurements used were of total column ozone (Orsolini *et al.*, 2003). The recent launch (in March 2002) of the European Space Agency (ESA) Envisat satellite has provided a wealth of new data on the seasonal evolution of the stratosphere, including the evolution of the distribution of tracers. The Michelson Interferometer for Passive Atmospheric Sounding (MIPAS) instrument aboard Envisat is particularly suited for height-resolved global studies of the summer stratosphere as it measures from Pole to Pole and has good-quality, height-resolved measurements from 200 hPa to 1 hPa of ozone and trace-gas species such as CH₄ and N₂O (Lahoz *et al.*, 2006; Raspollini *et al.*, 2006). The Microwave Limb Sounder (MLS) aboard the EOS Aura platform has also had this capability from August 2004 (Manney *et al.*, 2005b, 2006).

Height-resolved global ozone data from Envisat’s MIPAS, together with total column ozone global data from the Total Ozone Monitoring Spectrometer (TOMS) and meteorological data from the European Centre for Medium-range Weather Forecasts (ECMWF), have been recently used to study LOEs in the NH summer stratosphere (Orsolini and Nikulin, 2006). Only a few studies using trace-gas data have been done of the NH summer

* Correspondence to: W. A. Lahoz, Data Assimilation Research Centre, DARC, University of Reading, UK.
E-mail: swslahoz@reading.ac.uk

† Now at ECMWF, UK.

stratosphere: Manney *et al.* (2006) used ozone, N₂O, and H₂O global height-resolved data from EOS MLS; Durray and Hauchecorne (2005) used CH₄ and H₂O height-resolved *in situ* data from an infrared spectrometer.

A major motivation for studying the summer stratosphere is that changes in stratospheric ozone affect the radiation reaching the ground, and thus have an impact on human health and ecosystems (Orsolini *et al.*, 2003; Orsolini and Nikulin, 2006). In particular, summertime LOEs thin the ozone layer, and cause an enhancement of the erythemal UV dose at the ground (Orsolini *et al.* 2003). Other motivations for studying the summer stratosphere include assessing the relationship between springtime and summertime ozone (Fioletov and Shepherd, 2005), and improving our understanding of models of the atmosphere. As discussed by Orsolini (2001) and Manney *et al.* (2006), models of the summer stratosphere fail to reproduce some features of the summertime circulation, examples being the persistence of winter polar vortex fragments and FrIACs.

Crucial ingredients in studying summertime stratospheric ozone distributions are how the winter polar vortex breaks up and how the summertime high grows, and understanding the transport and photochemical processes affecting the ozone distribution. FrIACs can bring mid-latitude air to high latitudes; vortex break-up can produce vortex fragments that retain some features of the wintertime polar vortex, e.g. small amounts of trace gases such as CH₄ and N₂O (Manney *et al.*, 2005b for the Southern Hemisphere; Manney *et al.*, 2006 for the NH).

In the present paper, we use Envisat MIPAS data in the pressure range 200 hPa to 1 hPa to document and analyse the meteorological and trace-gas evolution of the stratosphere during NH summer 2003. Two features of our analysis are: (1) the adoption of a Pole-centred interpretation of the evolution; and (2) the use of ‘curtains’ of MIPAS data – sequences of vertical profiles along the viewing tracks of the instrument. The former feature helps interpret the data in a physically meaningful (coordinate-independent) way; the latter retains the information content of the data without the blurring effect of gridding by interpolation between viewing tracks, or averaging along latitude circles. By Pole-centred, we mean that the curtains of MIPAS data are centred about the Pole, with the emphasis on following the evolution of the stratospheric polar vortex and the summertime high. The Pole-centred approach has been applied successfully to the study of stratospheric winter in the NH and the Southern Hemisphere (SH; Lahoz *et al.*, 1994, 1996, 2006). To our knowledge, this approach has not been hitherto applied to the study of the summer stratosphere.

2. Method

The evolution of the NH summer is followed using Pole-centred stratospheric cross-sections of MIPAS ozone and trace-gas data for selected days over the period

April–November 2003. These days are chosen to capture dynamical features of particular interest. The Pole-centred view is complemented with meteorological data, viz. synoptic maps of geopotential height and time series of temperature and zonal winds from the Met Office troposphere–stratosphere analyses (Swinbank and O’Neill, 1994), and potential vorticity (PV) derived from ECMWF operational analyses (Simmons *et al.*, 2005).

2.1. MIPAS data

MIPAS is an interferometer for measuring infrared emissions from the atmospheric limb. MIPAS operational data are available between July 2002 and March 2004, after which instrument problems meant it could only be used occasionally. The operational measurements were made along 17 discrete lines-of-sight in the reverse of the flight direction of Envisat, with tangent heights between 8 km and 68 km. The spacing between measurements is ~3 km through the stratosphere, but larger above. MIPAS typically samples a volume ~3 km in the vertical, ~30 km in azimuth, and ~300 km along the line-of-sight. Precise values will differ slightly with species and between retrievals: the true vertical resolution is described by an averaging kernel (Rodgers, 2000). The approximate vertical resolution for the MIPAS measurements used in this paper is ~3 km. Envisat follows a sun-synchronous polar orbit, allowing MIPAS to sample globally, and to produce up to ~1000 atmospheric profiles a day. The approximate spacing between the measurements along the orbit track is ~3.5° latitude (~400 km). From the infrared spectra, ESA retrieves profiles of pressure, temperature, ozone (O₃), water vapour (H₂O), HNO₃, methane (CH₄), nitrous oxide (N₂O), and NO₂, at up to 17 tangent points (ESA, 2004).

In this paper we use MIPAS version 4.61 data, which has been evaluated under the auspices of ESA (<http://envisat.esa.int/workshops/acve2/contents.html>, accessed 8 December 2006), and in assimilation experiments at the Data Assimilation Research Centre (DARC; Geer *et al.*, 2006a, 2006b). At the Global Modeling Assimilation Office (GMAO; Wargan *et al.*, 2005), and at ECMWF (Dethof, 2003), earlier data versions were evaluated, but the results are similar. More recently, Raspollini *et al.* (2006) have evaluated the MIPAS level 2 products. Vertical oscillations have been reported in the MIPAS retrievals (Lahoz *et al.*, 2006; Raspollini *et al.*, 2006). These are sometimes found in the CH₄ data, but as can be seen in the figures of Lahoz *et al.*, oscillations do not persist from profile to profile, and the vertical frequency is that of the retrieval vertical grid. The figures in this work are largely unaffected, but tracer variations on the scale of a single level of one retrieval (appearing as a bullet point in the figures) should be treated with caution.

Of the long-lived tracers, we chose to focus on CH₄. Despite the vertical oscillation problem, it is of much better quality than the MIPAS H₂O observations (Lahoz *et al.*, 2006) and it has less missing data than

the N_2O fields. We did also examine the N_2O fields, and though we do not show them in the paper for brevity, they support the conclusions drawn from the CH_4 . For this paper, height-resolved profiles of ozone and CH_4 have been interpolated to isentropic levels and a basic screening procedure has been applied to remove bad data. We exclude duplicated profiles and those with unrealistic values of pressure; individual retrieval points are excluded if the mixing ratio or observational error is unrealistic (see Lahoz *et al.*, 2006 for further details). In the orbit cuts shown in section 3, the rejected observations can be identified by black areas in the figures.

2.2. Meteorological data

In this paper we use geopotential height and winds from the troposphere–stratosphere Met Office analyses (Swinbank and O'Neill, 1994), a well-established 15-year dataset (Figure 1). Although it might be desirable to use a single meteorological dataset, we chose to use PV fields from ECMWF because they are generated at much higher horizontal resolution (Simmons *et al.*, 2005).

Swinbank and O'Neill (1994) provided the original description of the troposphere–stratosphere Met Office analyses. Since November 2000, the assimilation algorithm has been changed to a three-dimensional variational (3D-Var) data assimilation method (Lorenc *et al.*, 2000).

The PV fields used in this paper are derived from the analyses produced by the ECMWF operational numerical weather prediction system (Simmons *et al.*, 2005). The analyses are produced using a multivariate, four-dimensional variational (4D-Var) data assimilation system with an assimilation window of 12 h.

Further details on the Met Office and ECMWF analyses (e.g. spatial and temporal resolution; treatment of ozone) can be found in Lahoz *et al.* (2006).

3. Analysis

We describe the following: (1) vortex break-up and the build-up of the summertime high; (2) tracer evolution from spring to autumn, with discussion of FrIACs, vortex fragments and W-shaped isopleths; and (3) a low ozone pool in the lower and mid-stratosphere.

3.1. Overview

The NH stratospheric summer of 2003 (April–September) was not unusual compared with the recent historical record (1991–2004; Figure 1). The zonal mean zonal winds at 61.25°N and 10 hPa were easterly from mid-April to late August; North Pole temperatures at 10 hPa were above 220 K from April to mid-September. The period during which the North Pole had higher zonal mean temperatures than midlatitudes (e.g. 45°N) spanned from early April to late August.

We first discuss the evolution of the stratospheric geopotential height field during the NH summer 2003, with particular reference to the 10 hPa level (Figure 2). By mid-April the vortex is weak at 10 hPa (Figure 2(a) and (b)) and at 1 hPa (not shown). On 16 April the vortex is split and displaced from the Pole (Figure 2(a)) and by 23 April (Figure 2(b)) it has been stretched out around the developing high. It continues to decay through April and May (Figure 2(c)–(f)), and eventually all signature of cyclonic circulations disappears by mid-June (Figure 2(g)). As the vortex weakens in the mid- and upper stratosphere during April–June (Figure 2(a)–(g)), the anticyclone grows, displaces the vortex off the Pole, and eventually becomes the summertime high and the dominant feature of the summertime stratospheric circulation from early June to August (Figure 2(g) and (h)). (We do not show a plot for July, but the synoptic situation is very similar to that shown for June and August.) During this period the anticyclone in the mid-

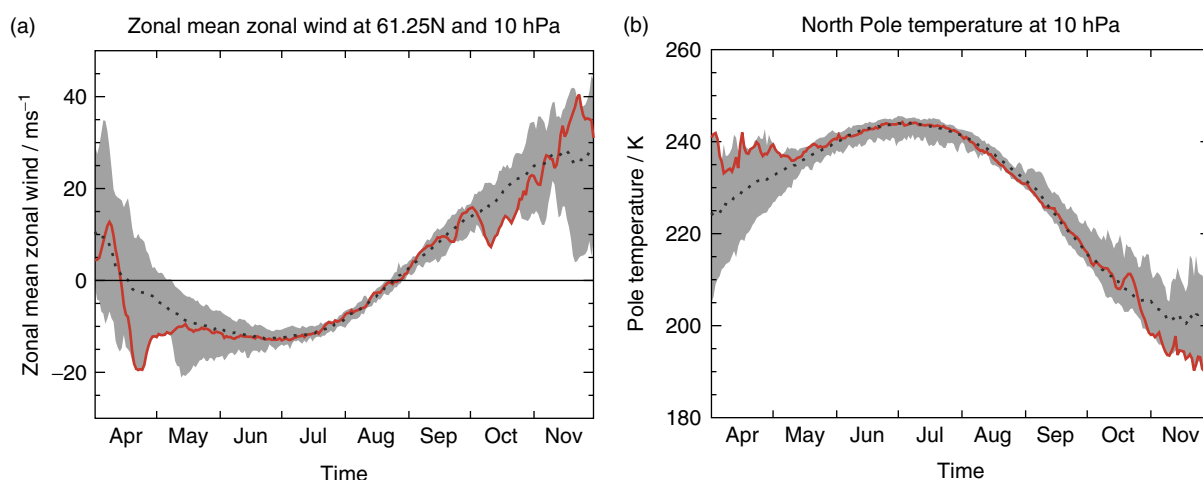


Figure 1. Time series of selected dynamical parameters for the NH stratospheric summer of 2003, April–November (solid/red lines): (a) zonally averaged zonal wind (m s^{-1}) at 61.25°N and 10 hPa (line marked is zero wind line; negative values correspond to easterly winds); (b) North Pole temperature (K) at 10 hPa. In both panels, the grey area shows the minimum and maximum range, and the dotted line the mean, of values for the period 1991–2004. Data produced by the Met Office. Figure courtesy of Carole Peubey. This figure is available in colour online at www.interscience.wiley.com/qj

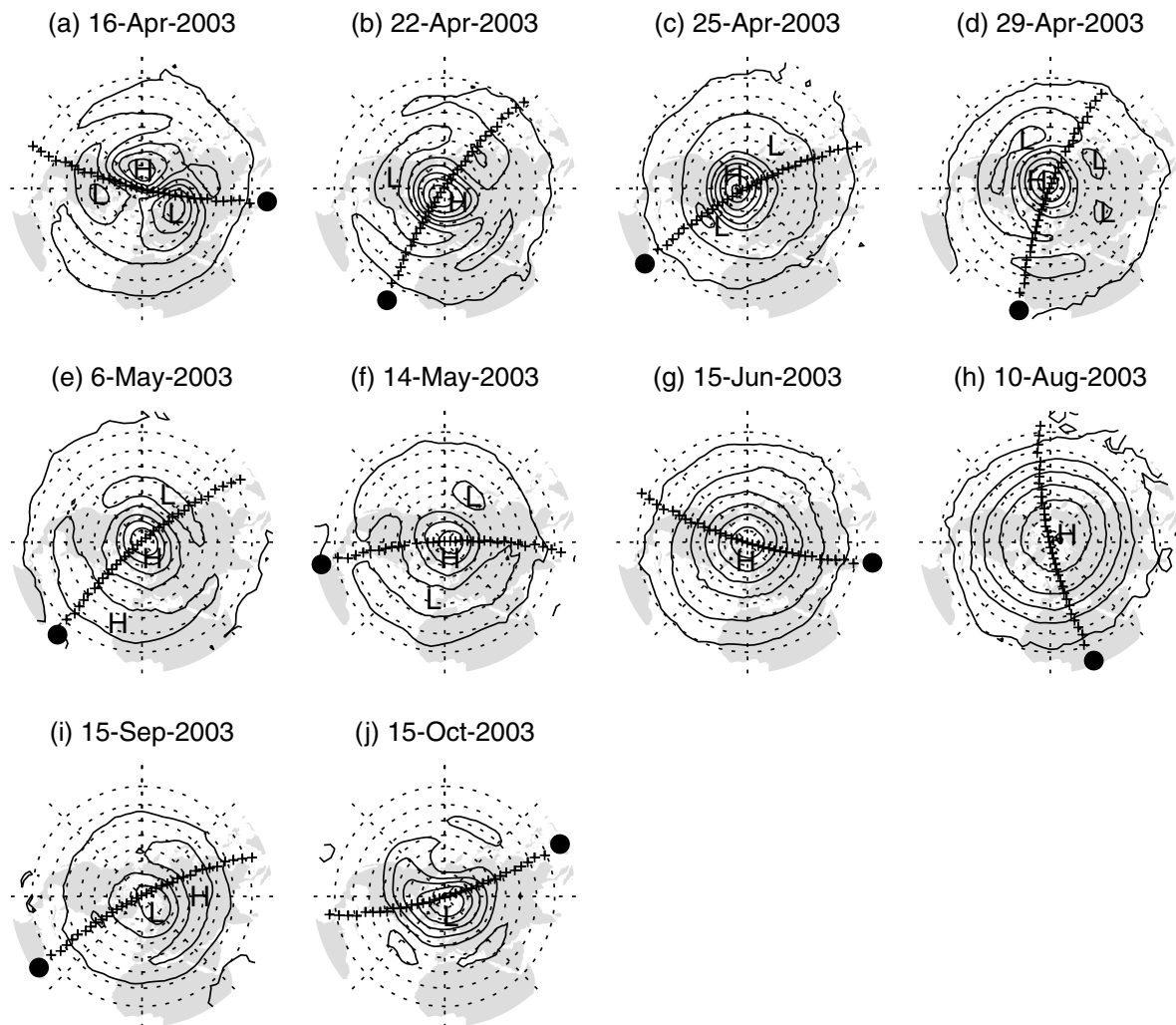


Figure 2. Geopotential height (m) at 10 hPa from Met Office stratospheric analyses with MIPAS viewing tracks of Figure 5 superimposed. The starting point of the viewing track is indicated by the solid circle. See Table I (Appendix) for the exact start times. Contours are spaced every 160 m. H and L indicate relatively high and relatively low pressure centres, respectively. Latitude circles are spaced every 10°, and a polar stereographic projection is used.

and upper stratosphere (10 hPa–1 hPa) evolves from being tilted westward with height and displaced off the Pole (mid-April), to being centred over the Pole, circular and barotropic (early June).

Summertime conditions remain until early September (not shown), when the wintertime vortex begins to build up in the upper stratosphere and the mid-stratosphere. By mid-September, the summertime high is weak and displaced off the Pole (Figure 2(i)). By mid-October (Figure 2(j)), the wintertime vortex is strengthening at 10 hPa, and is well established at 1 hPa (not shown).

In the lower stratosphere (e.g. 100 hPa), the polar vortex gradually becomes more distorted and weaker during the April–June period (not shown). After mid-June, as the vortex decays, the anticyclone grows and begins to encircle the weak vortex (located near the North Pole) reaching its greatest areal extent (almost encircling the vortex) by late August/early September. Although the polar vortex remains very weak in the lower stratosphere throughout the summer months (June–September), the cyclonic circulation only disappears above ~70 hPa, and

does not disappear at 100 hPa. After September, the vortex increases in size in the lower stratosphere with the onset of winter.

We now discuss the evolution of the summer by looking at monthly mean MIPAS CH₄ on isentropic levels, binned by latitude (Figure 3). Increased values at low latitudes indicate the tropical pipe, the ascending branch of the Brewer–Dobson circulation. Poleward of this, relatively low CH₄ values are indicative of air that has been longer in the stratosphere, and has descended from higher levels.

From April to July 2003, in the mid-and upper stratosphere (~700–2000 K), there are raised CH₄ values at high latitudes (poleward of ~70°N) relative to mid-latitudes (~40°N to ~70°N), with a maximum vertical extent in May. We examine this feature in detail later on, and it shows up in the Pole-centred cross-sections as a ‘W’ shape. It can be explained through the poleward transport of low-latitude air during the vortex break-up, and perhaps additionally, upward transport over the Pole owing to summertime diabatic heating. Through August

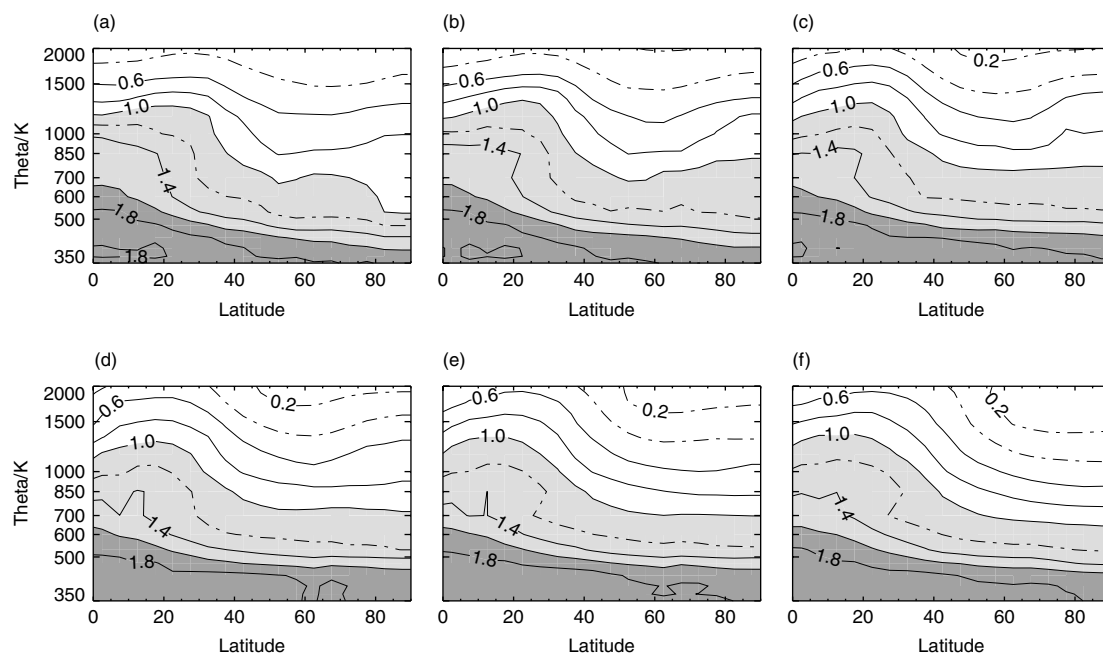


Figure 3. NH monthly mean MIPAS CH₄ data on isentropic levels and binned by latitude: (a) April 2003; (b) May 2003; (c) June 2003; (d) July 2003; (e) August 2003; (f) September 2003.

and September the raised CH₄ values at high latitudes relative to midlatitudes disappear, probably as a result of both isentropic mixing between these latitudes, and the onset of wintertime diabatic descent. The mechanisms discussed here (summertime diabatic heating, isentropic mixing) are discussed in more detail later in the paper.

In the lower stratosphere (below ~ 700 K), there tends to be less latitudinal variation in the zonal mean tracer amounts, indicative of stronger isentropic mixing between different latitudes, and relatively rapid poleward transport. As shown later in the paper, though the vortex break-up during April causes strong regional variability in lower-stratospheric CH₄ (not visible in these zonal means), it is removed by the beginning of May by the strong isentropic mixing at these levels.

Figure 4 shows MIPAS CH₄ binned by PV-equivalent latitude, derived from the ECMWF PV fields. This provides an alternative view of the vortex break-up in April and May. See Allen and Nakamura (2003) for a summary of the PV-equivalent latitude technique and its limitations. In Figure 4, high PV-equivalent latitudes correspond to the remnants of the winter vortex during April and May, and have low amounts of CH₄. A vortex edge is obvious in equivalent latitude at $\sim 70^\circ\text{N}$ at levels between 450 K and 850 K in April but not in May. As can be seen from Figure 2(b)–(f), through late April and May, the ‘vortex’ is in geographical terms a set of remnants located at latitudes 50°N – 60°N . As these vortex remnants become increasingly small, more of the high PV-equivalent latitude region corresponds to weakly higher PV coming over the Pole in the summer circulation. It is not possible to trace any possible vortex remnants into June with the PV-equivalent latitude technique; diabatic effects mean that PV is not conserved

over such long periods. Hence from June (Figures 3(c) and 4(c)) to September, the latitude and PV-equivalent latitude means are almost identical.

The CH₄ climatology of Randel *et al.* (1998), based on UARS data, does not show any significant elevation of spring/summer CH₄ values over the North Pole relative to midlatitudes, such as we see between April and July 2003 in the latitude means (part of what we call the ‘W’). There are a number of possible reasons for this. Firstly, Randel *et al.* used PV-equivalent latitude binning, and as indicated here by Figures 3 and 4, in April and May this would have largely prevented such a feature from being seen. In April and May, high PV-equivalent latitudes are largely representative of vortex remnants located geographically in the midlatitudes, rather than the Pole, where the increased CH₄ values are seen. Secondly, the Randel *et al.* climatology relies chiefly on Halogen Occultation Experiment (HALOE) data, which has very infrequent sampling of latitudes north of 60°N during the April–August period. These gaps were filled by Cryogenic Limb Array Etalon Spectrophotometer (CLAES) data, which were only available for the period January 1992 to April 1993. As discussed later, it may be that the ‘W’ does not occur every year. Prime causes of the W are the poleward transport of low-latitude air during the vortex break-up, and perhaps additionally, upward transport over the Pole due to summertime diabatic heating. FrIACS, associated with the former, contribute to a strong W signature, so if they do not occur, the W may not form. Manney *et al.* (2006) suggest that no FrIACs occurred in NH summer 1992. Hence the high-latitude NH summer in the Randel *et al.* climatology may well be representative of a year in which a W did not form.

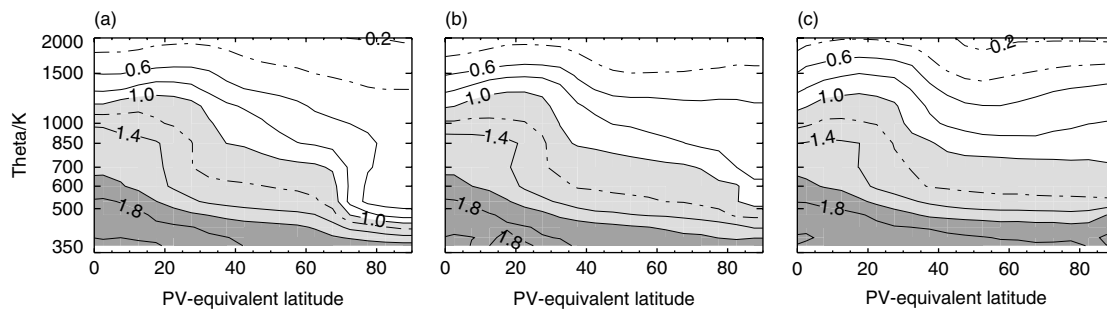


Figure 4. NH monthly mean MIPAS CH₄ data on isentropic levels and binned by PV-equivalent latitude: (a) April 2003; (b) May 2003; (c) June 2003. Results for July–September are nearly identical to those using latitude binning, so are not shown.

3.2. Tracer evolution

We first describe the evolution of tracers and PV for the period April–October 2003. We present ten CH₄ along-track vertical cross-sections ranging from 350 K to 2000 K and from 16 April to 15 October (Figure 5). We also present corresponding maps of ECMWF PV at 850 K (~ 10 hPa) (Figure 6). The viewing tracks overlaid in Figure 2 and Figure 6 correspond to those shown in Figure 5.

The tracer cross-sections and the PV fields document the break-up of the polar vortex and the build-up of the summertime high during April; the development of FrIACs and vortex fragments during April–June; the resulting transport causing, during May–August, a W-shape in the tracer isopleths in the mid- and upper stratosphere (see section 3.1); its later destruction; and the build-up of the polar vortex during September–October.

3.2.1. FrIACs

Using data from the EOS MLS from the NH spring and summer 2005, Manney *et al.* (2006) describe a mid-stratosphere FrIAC located between ~ 25 km and ~ 45 km, which remains coherent while being slowly advected around the North Pole by the prevailing high-latitude easterlies. The anticyclone contained air masses with H₂O and N₂O abundances characteristic of midlatitudes. Originating in the poleward transport of midlatitude air during the April final warming, the air masses confined in the anticyclone rotated around the Pole with a variable period of 2–3 weeks, before disappearing in August 2005. The ozone anomaly associated with the FrIAC was shorter lived owing to the relatively fast photochemical ozone relaxation. The anticyclonic anomaly was initially visible in the PV field, but this was not the case after June 2005.

Frozen-in vortex remnants (see later) have been reported in models (Hess, 1991; Orsolini, 2001) and observations (Hess and Holton, 1985; Durry and Hauchecorne, 2005; Manney *et al.*, 2005b). FrIACs can be regarded as the opposite of vortex remnants, as the former are long-lived anticyclonic vortices originating from low latitudes, whereas the latter are long-lived cyclonic vortices originating from high latitudes.

We now describe the evolution of an FrIAC seen in the 2003 CH₄ cross-sections and PV maps. The fidelity of the

FrIAC is given credibility by its signature appearing in both the MIPAS CH₄ and N₂O cross-sections, as well as in the PV fields (which are independent of the MIPAS data):

- (a) 16 April (Figures 5(a) and 6(a)): The tracer isopleths reflect the last stages of NH winter 2002–2003, as the vortex breaks up (Manney *et al.*, 2005a): (1) dipping of isopleths (see, e.g., the 1 ppmv isopleth) at high latitudes in the mid- and lower stratosphere, resulting from large-scale diabatic descent in the wintertime polar vortex; and (2) weak isentropic tracer gradients at midlatitudes in the mid- and upper stratosphere, associated with isentropic mixing of air masses as the vortex breaks up (profiles 3–9 and 22–26). The developing anticyclone (Figure 2(a)) has brought a broad tongue of low latitude, low PV air over the North Pole. The viewing track intersects this tongue, indicated by high CH₄ values, at ~ 500 K to ~ 1300 K, profiles 15–20. CH₄ values peak at ~ 1 ppmv in the centre of this (profiles 15–16, at ~ 850 K – ~ 1000 K), indicating relatively unmixed low-latitude (e.g. 30°N) air, which we will consider to denote the centre of the developing FrIAC. For 16 April and other selected dates below, other cross-sections that cut across the FrIAC reveal air with relatively low PV values and enhanced CH₄.
- (b) 22 April (Figures 5(b) and 6(b)): This date occurs during the final warming, when the polar vortex appears as an elongated high-PV tongue circling the midlatitudes. The FrIAC is identified as a small-size PV local minimum centred over northeast Greenland. It is embedded in the broad tongue of low PV air, which was advected poleward during the final warming. Near 850 K (over Greenland), and in the pressure range ~ 10 hPa to 3 hPa, the cross-section (profiles 15–17) reveals enhanced CH₄.
- (c) 25 April (Figures 5(c) and 6(c)): The FrIAC, as denoted by a minimum in the PV fields has progressed slightly westward and is now to the west of Greenland, and is seen to coincide with a high-latitude CH₄ enhancement at profiles 15–17.
- (d) 29 April (Figures 5(d) and 6(d)): The FrIAC maintains its westward progression in the PV fields, reaching the

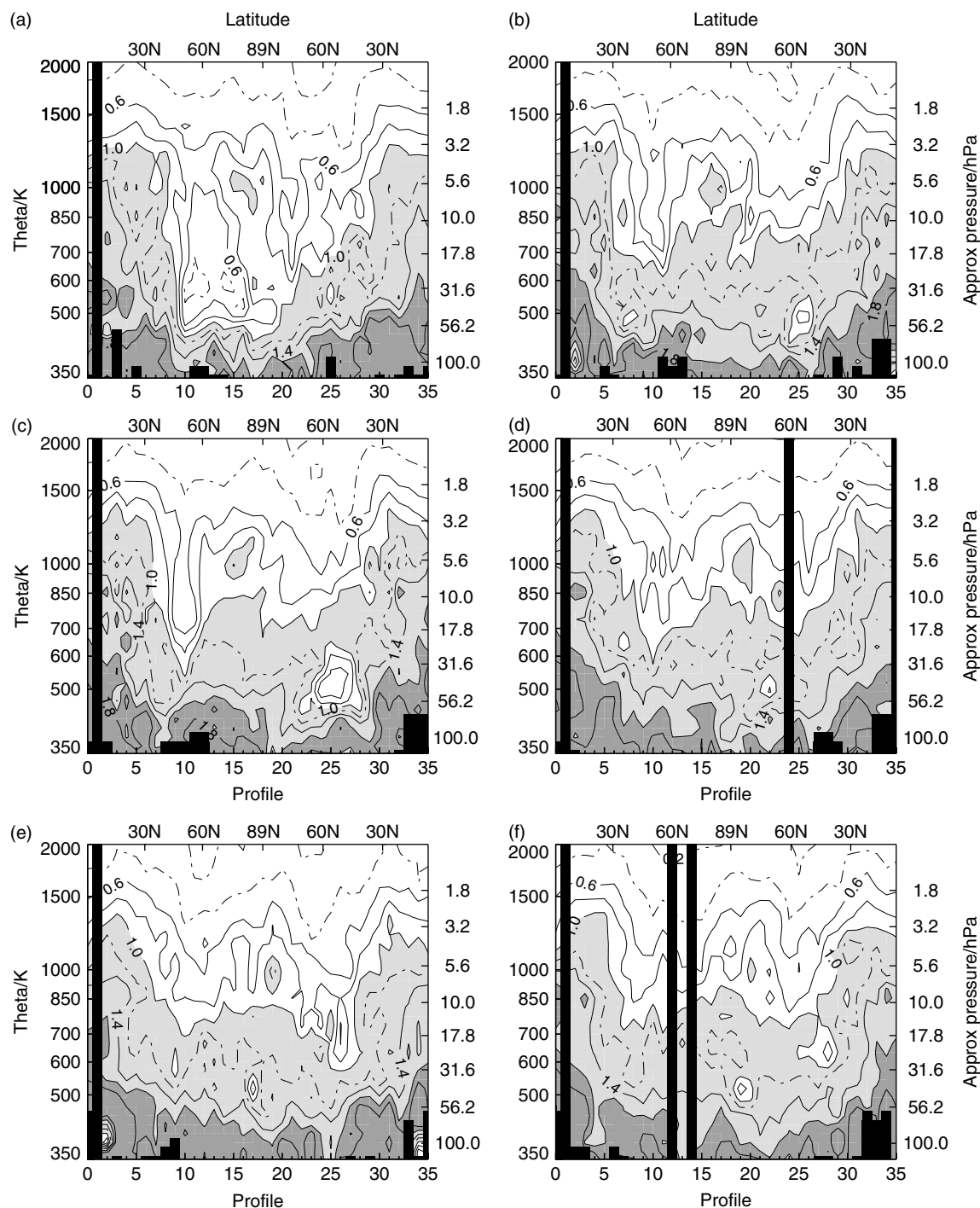


Figure 5. Orbit cuts for MIPAS CH₄ observations for (a) 16 April 2003; (b) 22 April 2003; (c) 25 April 2003; (d) 29 April 2003; (e) 6 May 2003; (f) 14 May 2003; (g) 15 June 2003; (h) 10 August 2003; (i) 15 September 2003; (j) 15 October 2003. Units are ppmv. The contour interval is 0.2 ppmv. White denotes values less than 1 ppmv. Darker shading indicates higher values. Black areas indicate missing data.

International Date Line, and continues to be associated with enhanced CH₄ (profiles 19–20).

(e) 6 May (Figures 5(e) and 6(e)): The PV minimum has moved slightly closer to the Pole and by May (not shown), it is nearly at the North Pole.

(f) 14 May (Figures 5(f) and 6(f)): The PV anomaly, now slightly smaller in size, is above the Russian Arctic coast (near 100°E), and the associated CH₄ anomaly at ~1000 K still has values comparable to those on 22 April (~1 ppmv; profile 20). By 22

May (not shown), while migrating further westward (the FrIAC is now near 100°W, over the Canadian Arctic), the distinctive signatures of the FrIAC (the PV minimum and the patch of CH₄ values greater than 1 ppmv) weaken further, though the surrounding area of relatively high CH₄ values persists.

Examination of the along-track cross-sections was not carried out immediately beyond 22 May, partly because of a MIPAS data gap from 24 May to 5 June. After 5 June,

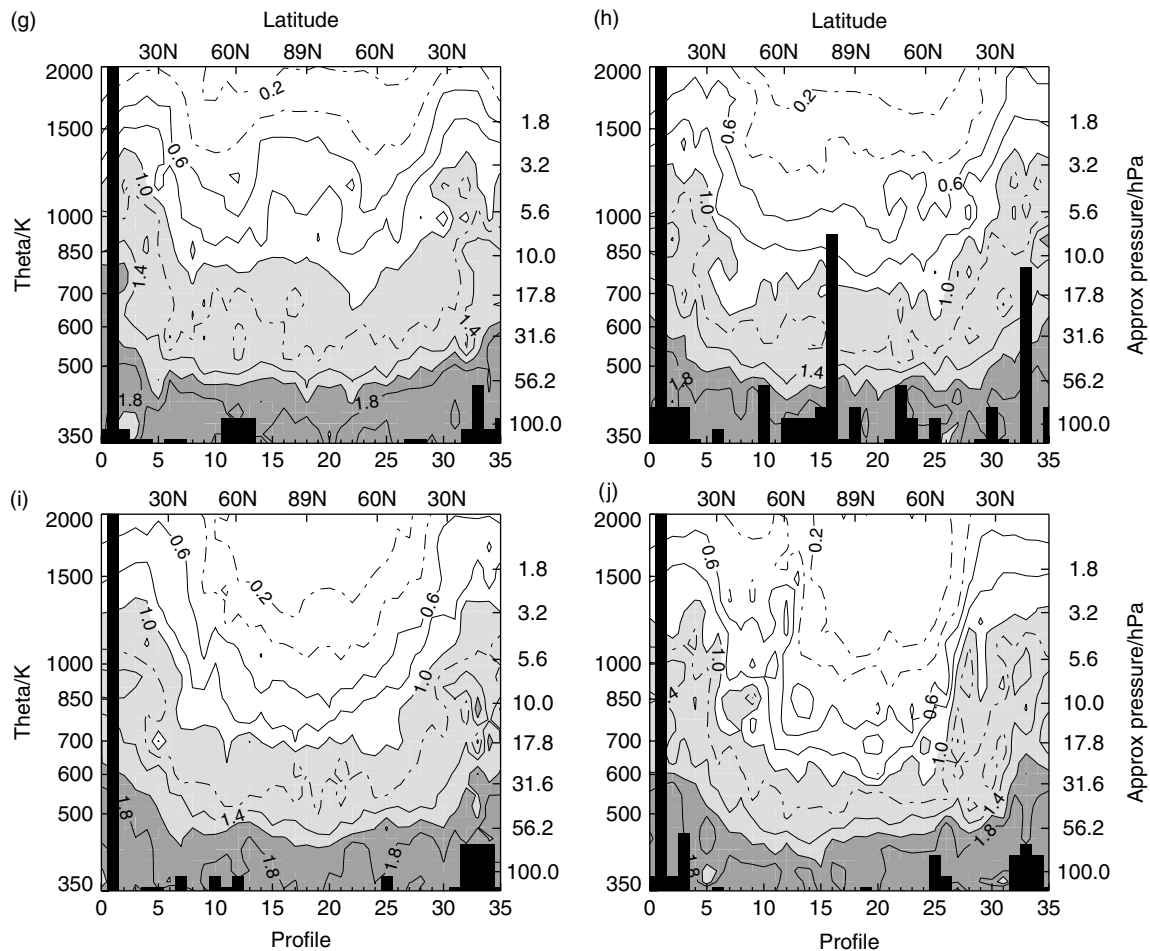


Figure 5. (Continued).

generally raised methane values persist over the North Pole until late July/early August at 850 K to 1000 K (over the period 31 July to 4 August the CH_4 isopleths become flat over the Pole), but the PV signature has entirely disappeared. As shown in Manney *et al.* (2006), the PV signature of the FrIAC can disappear before the CH_4 signature, presumably owing to diabatic effects; this disappearance may also be related to inaccuracies in wind and PV fields in the analyses near the summer Pole. EOS MLS observations during NH spring and summer 2005 allowed the identification of the FrIAC for over two months after the anomaly vanished in the analysed PV fields.

The tracer cross-sections and PV fields indicate only one clear-cut FrIAC event for 2003 (tracked from mid-April to mid-May – see above). Initially, the FrIAC and the broad tongue of anticyclonic air intruding into high latitudes are identical (Figures 5(a) and (b); 6(a) and (b)). Later, the pool of anticyclonic air reduces in size to a small-scale, westward propagating coherent vortex, embedded in the large-scale summertime high (Figures 5(c)–(f); 6(c)–(f)). This suggests that the dynamical contribution to the development of the summertime high from FrIAC incursions is relatively small.

Questions remain about the role such FrIAC events play in the chemical balance of the polar summer stratosphere. Midlatitude air brought to northernmost

latitudes will bring its own chemical signature (e.g. high O_3 , low H_2O , low NO_x/NO_y), and will experience large ozone loss as it undergoes chemical relaxation. In the same way that air confined in wintertime stratospheric anticyclones develops into low ozone pockets (Harvey *et al.*, 2004), the air masses confined in the FrIAC may retain characteristic chemical signatures differing from the ambient polar air, even if the latter is also drawn from midlatitudes (see Figure 5(b) for 22 April). However, the evidence from MIPAS suggests that ozone values in the FrIAC are less distinct from its surroundings than for the tracer fields (e.g. CH_4). This may be explained by the summer chemistry giving low ozone values where the FrIAC forms. The small areal extent of the FrIAC probably precludes its affecting strongly the polar chemical budget. We have here focused on the long-lived tracers (e.g. CH_4); some further analysis of the MIPAS chemically active species (e.g. NO_2) would be desirable. This is beyond the scope of this paper.

3.2.2. Long-lived vortex fragments

The CH_4 cross-sections also provide evidence for drifting vortex remnants after the break-up in April. For example, on 25 April, low CH_4 tongues are cut by the viewing track over Eastern Canada in the mid-stratosphere and

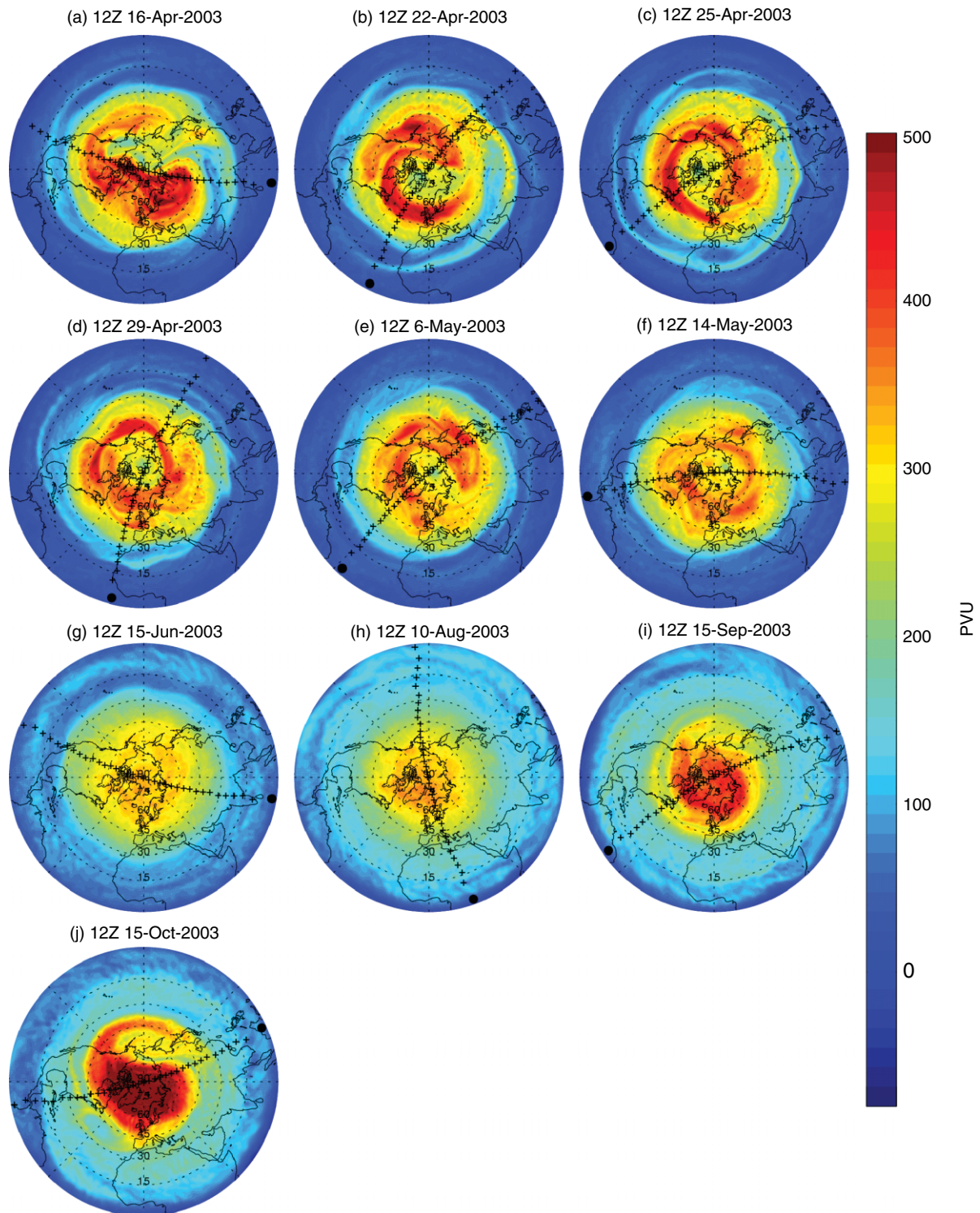


Figure 6. PV (PV units) at 850 K from ECMWF analyses for selected days from 16 April to 15 October 2003. The starting point of the viewing track associated with Figure 5 is indicated by the solid circle. The highest PV values are denoted by red and the lowest values by blue.

the North Pacific in the lower stratosphere (profiles 9–10 at ~ 700 – 1300 K; profiles 23–27 at 400 – 600 K in Figure 5(c)). Vortex CH_4 values of ~ 0.6 ppmv at 850 K in spring before the vortex break-up (Figure 5(a)) are consistent with values found in April 1993 during the ATMOS (Atmospheric Trace Molecule Spectroscopy) mission (Manney *et al.*, 1999). At 850 K, the accuracy and precision in ATMOS CH_4 measurements are each

$\sim 5\%$ (Abrams *et al.*, 1996); the total error in MIPAS CH_4 measurements is $\sim 10\%$ (Raspollini *et al.*, 2006). The difference in CH_4 values between the vortex fragment candidates and the surrounding air is larger than this, giving confidence that the MIPAS cross-sections do identify the signature of vortex fragments.

If we take the 0.6 ppmv or 0.8 ppmv isopleth as representative of an individual vortex fragment, these

fragments have almost disappeared from the 850 K level by early May (Figure 5(e)). However, this definition of an individual fragment is somewhat arbitrary, and we see that the vortex fragments have created an area of low CH₄ and high PV (Figure 6(e)) which persists long afterwards. These remaining regions of low CH₄ tend to be broader, are vertically aligned, and have weaker isentropic gradients than in April (Figure 5(e) and (f)). At levels below 600 K, there is virtually no sign of vortex remnants, at least at the scales clearly observable by MIPAS. A number of remaining low-CH₄ features (e.g. Figure 5(f), profile 19, 500 K) are so small that they are difficult to distinguish reliably from erroneous vertical oscillations (see section 2.1), but they still suggest that the vortex remnants are being broken into increasingly smaller pieces.

The faster disappearance of CH₄ anomalies below ~600 K, i.e. below the average altitude of the zero-wind line, is in agreement with Orsolini (2001), Konopka *et al.* (2003), and Manney *et al.* (2005b). Even in a summer westward flow regime with weak meridional shear, vortex remnants will get vertically sheared down to scales that are below the MIPAS retrieval resolution. In a study of the SH final warming in the spring of 2002 based on MIPAS observations, Orsolini *et al.* (2005) were able to track individual vortex remnants for about two weeks. In a study of SH winter 2003 based on MIPAS observations, Lahoz *et al.* (2006) were able to track a vortex filament for about three weeks. Our results, for the NH spring, are similar: if we start the clock on 16 April when the vortex started to split at 10 hPa, individual vortex fragments are becoming hard to track in MIPAS data by 29 April, again a period of about two weeks.

3.2.3. *W-shaped isopleths*

After vortex break-up, the tracer fields in the upper stratosphere become smoother, and by NH spring/early summer 2003 (late April–June) roughly zonally symmetric W-shaped tracer isopleths can be seen in the MIPAS CH₄ cross-sections (Figure 5(b)–(g)). The observed pattern is one of raised isopleths at high latitudes (the ‘core’ of the W), lowered isopleths at midlatitudes (the ‘moat’), and raised isopleths in the tropics (the ‘end-points’).

As shown in Figure 5(a), the W is not present during mid-April, when the isopleths mainly reflect the last stages of NH winter 2002–2003, as the vortex breaks up (Manney *et al.*, 2005a). Nevertheless, Figure 5(a) shows raised CH₄ values near the Pole associated with the developing anticyclone, particularly at ~1000 K (profiles 13–18). By late April a signature of the W (raised isopleths at high latitudes, lowered isopleths at midlatitudes) begins to emerge, albeit weakly, in the mid- and upper stratosphere (levels above ~600 K; Figure 5(b)–(d)). Other orbit cuts for these days (not shown) confirm the roughly zonally symmetric nature of this feature. By mid-May, the W is more prominent. During the period May–June it extends from ~850 to ~2000 K (~10 hPa to ~1 hPa; Figures 5(e)–(g)). By

August there is still a signature from ~1400 to ~2000 K (~2 hPa to ~1 hPa; Figure 5(h)), but it is weaker than for the period May–June. By September the W cannot be distinguished from observational noise (Figure 5(i)). By October, there is no W (Figure 5(j)); instead, the tracer isopleths reflect the signature of the polar vortex as it builds up in NH winter 2003–2004. A similar pattern was already seen in the means of Figure 3.

The poleward advection of midlatitude air during vortex break-up, associated with the observed FrIAC event, and the build-up of the summertime high, brings air with relatively high CH₄ and low PV values to high latitudes. From PV maps (not shown), these intrusions of midlatitude air extend from ~600 K to ~1500 K during late April, and from ~850 K to ~1500 K during May. In the mid- and upper stratosphere high latitudes this provides the core of the W (roughly profiles 15–20; Figure 5(e)–(g)). The surrounding midlatitude air is made up of a mixture of air originating from the vortex (vortex remnants) and the surf zone, and has relatively low CH₄ and N₂O values and high PV values. This provides the moat of the W (roughly profiles 9–13 and 23–25; Figure 5(e)–(g)). The end-points of the W are found in the tropics at the edge of the tropical pipe, where the ambient air has relatively high CH₄ and low PV values (roughly profiles 2–5 and 29–32; Figure 5(e)–(g)).

Climatological diabatic heating fields computed from ERA-40 analyses appropriate for June–August NH summer (p. 176 in ERA-40 2005) show for levels between ~1000 K and ~1600 K relatively weak diabatic ascent (~4 K day⁻¹) at midlatitudes, and relatively strong diabatic ascent at low latitudes and high latitudes (~10 K day⁻¹). This differential diabatic heating might contribute to the W by raising the core and end-points with respect to the moat.

The height extent of the midlatitude intrusions toward the Pole seen during April–May provides clues toward discriminating between the relative importance of poleward transport and diabatic heating in forming the W. These intrusions span a region of relatively strong diabatic heating (~1000 K to ~1500 K), and a region of relatively weak diabatic heating (~700 K to ~1000 K). This suggests that poleward transport is more important than diabatic heating in the mid-stratosphere, levels between ~700 K and ~1000 K. However, we cannot tell which of these processes is more important for levels above ~1000 K. FrIACs, which are a manifestation of poleward transport, have the strongest signature for levels between ~850 K and ~1000 K (see Figure 5). For levels between ~700 K and ~850 K, where poleward transport is expected to dominate (see above), there is no clear-cut signature of a FrIAC, either in the cross-sections or in the PV maps (see discussion on FrIACs in section 3.2). Though the FrIAC is not so clear-cut at 700–850 K, transport must still be the main cause of the W at these levels.

The MIPAS trace-gas data show that the moat of the W extends down to ~600 K in mid-April (Figure 5(b)

and (c)) and then gradually rises monotonically to ~ 850 K in mid-May (Figure 5(f)) and ~ 900 K in mid-June (Figure 5(g)). The steady rising of the moat between mid-April and mid-June might be due to the gradual erosion of vortex remnants during this period. Support for this hypothesis is provided by PV maps for levels 530–1000 K (not shown), which suggest that the lowest level at which individual vortex fragments can still be discerned rises progressively during the period. The lack of a W in the lower stratosphere during NH summer could be due to strong isentropic mixing between high and midlatitudes. Relatively weaker diabatic heating rates are unlikely to counteract this: in the lower stratosphere, mid- and high-latitude diabatic heating is small, varying from ~ -2 K day $^{-1}$ to ~ 2 K day $^{-1}$ (p. 176 in ERA-40, 2005).

The persistence of the W in the mid- and upper stratosphere into July and August is in accord with studies showing very weak isentropic mixing here. Allen and Nakamura (2001) use UK Met Office winds and effective diffusivity to investigate isentropic mixing in the stratosphere (levels between 350 K and 1900 K). In the NH, in the mid- and upper stratosphere, at 850 K and 1900 K, they see strong mixing in May and June, a minimum of mixing in July and August, and increasing mixing in September and October (see their plate 1). Mixing extends over a broad region from high latitudes to the sub-Tropics. Their general result is that at these levels mixing is strong during the transition in wind regimes occurring in spring and autumn, and weak during the summer, when the critical wind line descends and shuts off upward Rossby wave propagation. One has to conclude from these results of Allen and Nakamura that mixing is sluggish in the NH summer upper stratosphere polar regions. Similar results to those of Allen and Nakamura are shown by Haynes and Shuckburgh (2000) and Wagner and Bowman (2000), though they only investigate levels up to 950 K, and in contrast to the other papers, Wagner and Bowman find relatively strong isentropic mixing for levels between 550 K and 950 K in August.

In the lower stratosphere (460 K), Allen and Nakamura (2001) see strong extratropical mixing in the NH over the period May–October (see their plate 1). This comes from stirring by the top of eddies extending from the troposphere, but the upward extension of the tropospheric jet only allows the mixing to take place at midlatitudes and high latitudes (Piani *et al.*, 2002). Haynes and Shuckburgh (2000) and Wagner and Bowman (2000) also show strong extratropical mixing through the summer in the lower stratosphere. This strong mixing is consistent with the lack of a W in the lower stratosphere (see Figure 5).

In the upper stratosphere, as NH summer advances, the W weakens and disappears (Figure 5(h) and (i)). A crucial question, which this paper cannot answer, is whether this is mainly owing to continued (and enhanced compared with April–June) isentropic mixing between the Pole and surrounding areas, or whether it

is mainly owing to the onset of wintertime large-scale diabatic descent as NH summer advances. Although the study of Allen and Nakamura (2001) discussed above indicates that isentropic mixing is sluggish in the upper stratosphere during July and August, there is a possibility that with enough time this mixing might help destroy the W.

Figures 3 and 4 suggest the possibility of mean diabatic descent in the NH polar stratosphere after June: the 0.6 ppmv contours of MIPAS CH $_4$ monthly means descend by ~ 300 K over the period June–August (from ~ 1300 K to ~ 1000 K). However, the lowering of the tracer isopleths might have been accomplished by isentropic mixing between polar air and midlatitude air.

PV fields at 850 K and above appear to show very little large-scale mixing during the period June–August 2003 (Figure 6(g)–(i) and others, not shown). At 850 K, PV filaments indicative of large-scale mixing only appear in September (Figure 6(j)). This would suggest that the weakening and eventual disappearance of the W in July and August may be mainly due to the onset of diabatic descent, rather than persistent, but sluggish, isentropic mixing. However, the balance between mixing and diabatic descent remains an open question.

3.3. Low ozone pool

MIPAS O $_3$ Pole-centred cross-sections show a low O $_3$ pool in the high-latitude NH summer stratosphere during 2003. The transition from low ozone values in the spring polar vortex to low ozone values in the summertime high, reflects the transfer of control of the ozone distribution from transport processes to photochemical processes. Figure 7 shows the evolution of ozone during NH summer 2003 for selected days. Figures 2 and 6 show the location of the cross-sections.

The two lobes of the polar vortex on 16 April (Figure 2(a)) contain relatively ozone-poor air: profiles 10–15 and 20–23 in Figure 7(a) for, respectively, the lobe over Eurasia and the lobe over North America. However, low O $_3$ values only extend up to ~ 700 K (~ 20 hPa), and in particular, the intrusion of subtropical air (Figure 6(a); Figure 7(a) profiles 10–15, 700–1000 K), associated with the development of the summer anticyclone, contains relatively high O $_3$ amounts.

When the summertime high becomes dominant, the latitudinal extent of the low O $_3$ pool is typically poleward of 60° N, although this varies with isentropic level (the low O $_3$ pool is broader at 600 K than at 700 K; see Figure 7(b) and (c)). Associated with the summertime high, MIPAS ozone cross-sections show a low O $_3$ pool (values less than 5 ppmv) in the high-latitude stratosphere (~ 450 – 1000 K; profiles 10–25; Figure 7(b) and (c)). During summer, photochemical processes control the ozone distribution, as large regions of the high-latitude stratosphere receive uninterrupted sunlight for many weeks. This causes ozone loss through catalytic cycles (NO $_x$ – upper and mid-stratosphere; HO $_x$ – lower

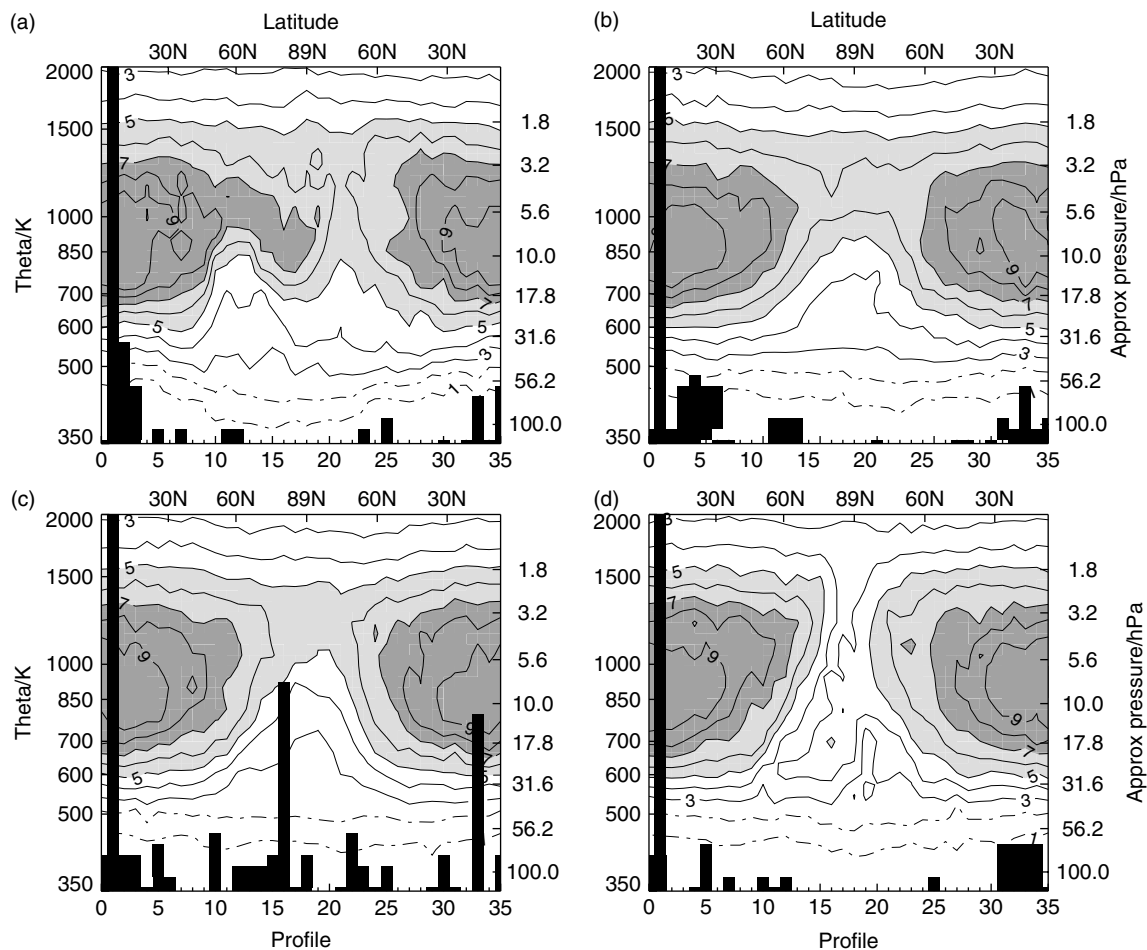


Figure 7. Orbit cuts for MIPAS ozone observations: (a) 16 April 2003; (b) 15 June 2003; (c) 10 August 2003; (d) 15 September 2003, with viewing tracks as Figure 2. Units are ppmv. The contour interval is 1 ppmv. White denotes values less than 5 ppmv. Darker shading indicates higher values. Black areas indicate missing data.

stratosphere; e.g. Park and Russell, 1994; Harvey *et al.*, 2004).

Transport processes (isentropic transport and diabatic heating) are only likely to play a minor role in the summer low ozone pool, but would reinforce the ozone distribution determined from photochemical processes. Isentropic transport would tend to bring relatively ozone-rich air from low latitudes to high latitudes in the mid- and upper stratosphere. Higher diabatic ascent in the high-latitude mid- and upper stratosphere (ERA-40, 2005), would tend to bring relatively ozone-poor air to the mid-stratosphere and relatively ozone-rich air to the upper stratosphere. In the lowermost stratosphere (below 500 K), mixing would tend to bring together air masses of similar O_3 content.

Meridional displacements of the stratospheric low ozone pool can be associated with LOEs, i.e. sudden decreases of the ozone column at mid- or high latitudes. This occurs when a region of low ozone in the mid-stratosphere sits on top of an anticyclonic ridge and, thus, a high tropopause (Orsolini *et al.*, 2003). Hence, the low stratospheric ozone values aloft accentuate the column ozone lowering caused by the ridging. Orsolini and Nikulin (2006) studied such an LOE during August

2003 using MIPAS data. Meridional displacements of low ozone air from high latitudes have been documented by Hoppel *et al.* (1999) using POAM (Polar Ozone and Aerosol Measurement) data. Hoppel *et al.* also find evidence for persistent large-scale ozone patterns at high latitudes that progress westward with the zonal mean wind.

The latitudinal extent of the low ozone pool remains roughly constant until September, when, still associated with the summertime high, it decreases in size, now extending poleward of $\sim 65^\circ N$ at ~ 700 K (Figure 7(d)). As winter progresses, the low O_3 pool, now associated with the polar vortex, remains confined to high latitudes.

During September–October (see Figures 5(i) and (j); 6(i) and (j)), as the NH winter polar vortex builds up, and dynamical processes increasingly control the O_3 distribution, the relatively low O_3 values extend throughout the stratosphere (350–2000 K; ~ 100 hPa to ~ 1 hPa) at high latitudes (Figure 7(d)). Between August and September, O_3 values in this region decrease from 5–6 ppmv to ~ 4 ppmv. Both photochemical processes and diabatic descent are likely to contribute to this change.

With the onset of winter, large-scale diabatic descent brings ozone-poor air from the uppermost stratosphere and mesosphere to the mid- and upper stratosphere at high

latitudes in the vortex. Methane cross-sections for the period August–October (Figure 5(h)–(j)) suggest a diabatic descent of the 0.2 ppmv isopleths of ~ 300 K (from ~ 1800 K to ~ 1500 K) between August and September, and of ~ 400 K (from ~ 1500 K to ~ 1100 K) between September and October. The latitude and PV-equivalent latitude monthly means for CH_4 (Figures 3 and 4) also suggest similar diabatic descent. Note, however, as discussed in section 3.2, the lowering of the tracer isopleths might have been accomplished by isentropic mixing between polar air and midlatitude air (see also Figures 3 and 4).

4. Conclusions

In this paper we have used MIPAS trace-gas cross-sections, complemented by Met Office geopotential height fields and ECMWF PV maps, to study the structure and evolution of the NH summer stratosphere. Two features of our analysis are: (1) the adoption of a Pole-centred interpretation of the evolution; and (2) the use of ‘curtains’ of MIPAS data – sequences of vertical profiles along the viewing tracks of the instrument. This approach has hitherto not been applied to study the summer stratosphere.

This study provides a holistic picture of the evolution of the NH summer stratosphere in 2003, showing the close links between several distinctive phenomena. We start with the vortex break-up in April. As the vortex is displaced off the Pole, it fragments and the remnants are stretched out into a ring around the Pole at $\sim 50^\circ\text{N}$. These vortex remnants can be identified by relatively low CH_4 values and relatively high PV values. Also during the break-up, as high pressure moves over the Pole and starts to build, tongues of low-latitude air are drawn into the polar regions. This air has relatively low PV and high CH_4 values. This air remains in the region of the Pole, forming a FrIAC like that seen by Manney *et al.* (2006) in NH Summer 2005. As the summer moves on, there is a gradual smoothing (through mixing) of previously distinct features: the amplitude of CH_4 variations between the vortex remnants and the FrIAC is lessened.

From May to August, the mid- and upper stratosphere (700–2000 K) tracer isopleths display a W shape. By this, we mean that there are higher values of CH_4 over the Pole than at midlatitudes. The Pole (the ‘core’ of the W) is surrounded by a ring of air with relatively low CH_4 amounts (the ‘moat’). CH_4 amounts rise again at equatorial latitudes in the tropical pipe, forming the ‘end-points’ of the W. The main reason for formation of the W is the movement of air during vortex breakdown in April and May: there is poleward transport of midlatitude air, with which the FrIAC is associated; vortex air (often in the form of vortex fragments) is moved to the midlatitudes. However, above 1000 K, differential diabatic ascent may also be a contributing factor: faster ascent over the Pole than at midlatitudes will tend to raise the core of the W compared with the moat.

During the vortex break-up (April and May), PV anomalies are linked with CH_4 anomalies, but the link between PV and CH_4 is removed by the beginning of June, presumably by diabatic effects or by inaccuracies in assimilated wind fields. The W in the tracer isopleths persists much longer, before weakening and disappearing at progressively higher levels. At 850 K, the W persists through May and June. At 1000 K it persists through July and above 1500 K, a slight W persists until the end of August. The onset of NH wintertime diabatic descent starts to cause a dip in tracer isopleths at high latitudes from September onwards, as the vortex starts to build.

The maintenance and final destruction of the W are indicative of the strength of isentropic mixing in the NH summer stratosphere. No W is found below 700 K; vortex fragments are quickly destroyed in April by the strong isentropic mixing of the lower stratosphere. The persistence of the W at levels above 700 K is indicative of sluggish isentropic mixing in the mid- and upper stratosphere during the summer, supporting the conclusions of, among others, Allen and Nakamura (2001), which were based on assimilated wind fields. It is not clear, however, if the W is finally destroyed by continued slow isentropic mixing or by the onset of wintertime diabatic descent.

To our knowledge these W-shaped isopleths have not been previously observed, as might be expected given the lack of tracer observations at very high latitudes before the launches of Envisat and EOS Aura. As mentioned above, a main contributing factor to the formation of a W is the poleward transport of midlatitude air, e.g., in a FrIAC. Manney *et al.* (2006) point out that FrIACs may not be an annual phenomenon. Hence W-shaped isopleths may not be either. In the MIPAS data (available between July 2002 and March 2004), we have seen a W in the NH summer of 2002 (identified as a candidate for FrIACs by Manney *et al.*), but not in the SH summers of 2002–2003 and 2003–2004.

This study also showed observations of the low ozone pool that forms over the Pole in the summer stratosphere. As the summertime high becomes dominant during June–August, net photochemical O_3 loss produces a low ozone pool in the lower and mid-stratosphere. Finally, as the summertime high decays and the wintertime polar vortex builds up from September onwards the low ozone pool extends vertically throughout the stratosphere.

We see that the NH summer stratosphere distribution of trace gases and O_3 at mid- and high latitudes as measured by MIPAS can be generally explained by the interplay between transport and photochemical processes. This gives us confidence in the MIPAS data and in our broad understanding of NH summer stratosphere processes. Nevertheless, the MIPAS trace-gas data suggest that further studies are needed to answer the following questions:

- Are W-shaped isopleths a regular phenomenon?

- What is the association between the W-shaped isopleths and the FrIAC events?
- Is the W destroyed by isentropic mixing, or the onset of diabatic descent?
- Are W-shaped isopleths ever present in the SH?

Answering these questions will form part of future work on the summer stratosphere. Future work will also quantify some of the processes involved, and extend this approach to the SH summer stratosphere.

Acknowledgements

The NERC-funded Data Assimilation Research Centre (DARC; <http://darc.nerc.ac.uk>, accessed 8 December 2006) funds WAL; AJG was funded by the EU project ASSET (<http://darc.nerc.ac.uk/asset>, accessed 8 December 2006); YJO is funded by the Norwegian Research Council (AEROZKLIM project). COST 723 (<http://www.cost723.org>, accessed 8 December 2006) funded a visit by WAL to YJO to discuss the paper and write an earlier version. We thank Gloria Manney for discussions on FrIACs; Andrew Charlton for providing maps of complementary meteorological data; two reviewers for comments that helped improve the paper; and the Associate Editor for valuable suggestions.

Appendix

Table I. Exact starting times of the MIPAS viewing tracks shown in Figures 2 and 5–7.

Date of cross-section	Time of start of viewing track/UT
16 April 2003	16:42:36
22 April 2003	00:08:08
25 April 2003	01:54:17
29 April 2003	23:16:23
6 May 2003	01:08:27
14 May 2003	03:37:51
15 June 2003	16:56:47
10 August 2003	20:58:24
15 September 2003	02:20:22
15 October 2003	14:41:47

References

Abrams MC, Chang AY, Gunson MR, Abbas MM, Goldman A, Irion FW, Michelsen HA, Newchurch MJ, Rinsland CP, Stiller GP, Zander R, 1996. On the assessment and uncertainty of atmospheric trace gas burden measurements with high resolution infrared solar occultation spectra from space by the ATMOS experiment. *Geophys. Res. Lett.* **23**: 2337–2340.

Allen DR, Nakamura N, 2001. A seasonal climatology of effective diffusivity in the stratosphere. *J. Geophys. Res.* **106**: 7917–7935.

Allen DR, Nakamura N, 2003. Tracer equivalent latitude: a diagnostic tool for isentropic transport studies. *J. Atmos. Sci.* **60**: 287–304.

Dethof A, 2003. Assimilation of ozone retrievals from the MIPAS instrument onboard ENVISAT. *ECMWF Tech Memo* 428.

Duray G, Hauchecorne A, 2005. Evidence for long-lived polar vortex air in the mid-latitude summer stratosphere from in situ laser diode CH₄ and H₂O measurements. *Atmos. Chem. Phys.* **5**: 1467–1472.

ERA-40, 2005. ECMWF Re-Analysis. Project Report Series: 19. ERA-40 Atlas. P. Kållberg, P. Berrisford, B. Hoskins, A. Simmons, S. Uppala, S. Lamy-Thépaut, R. Hine. Available from <http://www.ecmwf.int/publications> (accessed 8 December 2006).

European Space Agency, 2004. *MIPAS Product Handbook*, issue 1.2, available from <http://envisat.esa.int/dataproducts/> (accessed 8 December 2006).

Fahey DW, Ravishankara AR, 1999. Summer in the stratosphere. *Science* **285**: 208–210.

Fioletov VE, Shepherd TG, 2005. Summertime total ozone variations over middle and polar latitudes. *Geophys. Res. Lett.* **32**: 10.1029/2004GL022080. Available at <http://www.agu.org/pubs/crossref/2005/2004GL022080.shtml> (accessed 8 December 2006).

Froidevaux L, Waters JW, Read WG, Elson LS, Flower DA, Jarnot RF, 1994. Global ozone observations from the UARS MLS: an overview of zonal-mean results. *J. Atmos. Sci.* **51**: 2486–2866.

Geer AJ, Lahoz WA, Bekki S, Bormann N, Errera Q, Eskes HJ, Fonteyn D, Jackson DR, Juckes MN, Massart S, Peuch V-H, Rharmili S, Segers A, 2006a. The ASSET intercomparison of ozone analyses: method and first results. *Atmos. Chem. Phys. Discuss.* **6**: 5445–5474.

Geer AJ, Peubey C, Bannister B, Brugge R, Jackson DR, Lahoz WA, Migliorini S, O'Neill A, Swinbank R, 2006b. Assimilation of stratospheric ozone from MIPAS into a global general circulation model: the September 2002 vortex split. *Q. J. R. Meteorol. Soc.* **132**: 231–257.

Harvey VL, Pierce RB, Hitchman MH, Randall CE, Fairlie TD, 2004. On the distribution of ozone in stratospheric anticyclones. *J. Geophys. Res.* **109**: 10.1029/2004JD004992. Available at <http://www.agu.org/pubs/crossref/2004/2004JD004992.shtml> (accessed 8 December 2006).

Haynes PH, Shuckburgh E, 2000. Effective diffusivity as a diagnostic of atmosphere transport. 1. Stratosphere. *J. Geophys. Res.*, **105**: 22777–22794.

Hess PG, 1991. Mixing processes following the final stratospheric warming. *J. Atmos. Sci.* **48**: 1625–1641.

Hess PG, Holton JR, 1985. The origin of temporal variance in long-lived trace constituents in the summer stratosphere. *J. Atmos. Sci.* **42**: 1455–1463.

Hoppel KW, Bowman KP, Bevilacqua RM, 1999. Northern Hemisphere summer ozone variability observed by POAM II. *Geophys. Res. Lett.* **26**: 827–830.

Konopka P, Groos JU, Bausch S, Muller R, McKenna DS, Morgenstern O, Orsolini Y, 2003. Dynamics and chemistry of vortex remnants in late Arctic spring 1997 and 2000: simulation with the Chemical Lagrangian Model of the Stratosphere (CLaMS). *Atmos. Chem. Phys.* **3**: 839–849.

Lahoz WA, O'Neill A, Carr ES, Harwood RS, Froidevaux L, Read WG, Waters JW, Kumer JM, Mergenthaler JL, Roche AE, Peckham GE, Swinbank R, 1994. Three-dimensional evolution of water vapour distributions in the Northern Hemisphere stratosphere as observed by the microwave limb sounder. *J. Atmos. Sci.* **51**: 2914–2930.

Lahoz WA, O'Neill A, Heaps A, Pope VD, Swinbank R, Harwood RS, Froidevaux L, Read WG, Waters JW, Peckham GE, 1996. Vortex dynamics and the evolution of water vapour in the stratosphere of the Southern Hemisphere. *Q. J. R. Meteorol. Soc.* **122**: 423–450.

Lahoz WA, Geer AJ, O'Neill A, 2006. Dynamical evolution of the 2003 Southern Hemisphere stratospheric winter using Envisat trace-gas observations. *Q. J. R. Meteorol. Soc.* **132**: 1985–2008.

Lorenz AC, Ballard SP, Bell RS, Ingleby NB, Andrews PLF, Barker DM, Bray JR, Clayton AM, Dalby TD, Li D, Payne TJ, Saunders FW, 2000. The Met. Office global three-dimensional variational data assimilation scheme. *Q. J. R. Meteorol. Soc.* **126**: 2991–3012.

Luo M, Park JH, Lee KM, Russell III JM, Bruehl C, 1997. An analysis of HALOE observations in summer high latitudes using air mass trajectory and photochemical model calculations. *J. Geophys. Res.* **102**: 16145–16156.

Manney GL, Michelsen HA, Santee ML, Gunson MR, Irion FW, Toon GC, Roche AE, Livesey NJ, 1999. Polar vortex dynamics during spring and fall diagnosed using trace gas observations from the Atmospheric Trace Molecule Spectroscopy Experiment. *J. Geophys. Res.* **104**: 18841–18866.

Manney GL, Krüger K, Sabutis JL, Sena SA, Pawson S, 2005a. The remarkable 2003–2004 winter and other recent warm winters in the Arctic stratosphere since the late 1990s. *J. Geophys. Res.* **110**: 10.1029/2004JD005367. Available at

- <http://mls.jpl.nasa.gov/joe/nh2003-04var-ppb.pdf> (accessed 8 December 2006).
- Manney GL, Santee ML, Livesey NJ, Froidevaux L, Read WG, Pumphrey HC, Waters JW, Pawson S, 2005b. EOS microwave limb sounder observations of the Antarctic polar vortex breakup in 2004. *Geophys. Res. Lett.* **32**: 10.1029/2005GL022823. Available at <http://www.agu.org/pubs/crossref/2005/2005GL022823.shtml> (accessed 8 December 2006).
- Manney GL, Livesey NJ, Jimenez CJ, Pumphrey HC, Santee ML, MacKenzie IA, Waters JW, 2006. EOS microwave limb sounder observations of "frozen-in" anticyclonic air in Arctic summer. *Geophys. Res. Lett.* **33**: 10.1029/2005GL025418. Available at <http://www.agu.org/pubs/crossref/2006/2005GL025418.shtml> (accessed 8 December 2006).
- Orsolini YJ, 2001. Long-lived tracer patterns in the summer polar stratosphere. *Geophys. Res. Lett.* **28**: 3855–3858.
- Orsolini YJ, Eskes H, Hansen G, Hoppe U-P, Kylling A, Kyrö E, Notholt J, van der A R, von der Gathen P, 2003. Summertime low-ozone episodes at northern high latitudes. *Q. J. R. Meteorol. Soc.* **129**: 3265–3275.
- Orsolini YJ, Randall CE, Manney GL, Allen DR, 2005. An observational study of the final breakdown of the Southern Hemisphere stratospheric vortex in 2002. *J. Atmos. Sci.* **62**: 735–747.
- Orsolini YJ, Nikulin G, 2006. A low-ozone episode during the European heat wave of August 2003. *Q. J. R. Meteorol. Soc.* **132**: 667–680.
- Park JH, Russell III JM, 1994. Summer polar chemistry observations in the stratosphere made by HALOE. *J. Atmos. Sci.* **51**: 2903–2913.
- Piani C, Norton WA, Iwi AM, Ray EA, Elkins JW, 2002. Transport of ozone-depleted air on the breakup of the stratospheric polar vortex in spring/summer 2000. *J. Geophys. Res.* **107**: 10.1029/2001JD000488.
- Randel WJ, Wu F, Russell JM, Roche A, Waters JW, 1998. Seasonal Cycles and QBO Variations in Stratospheric CH₄ and H₂O Observed in UARS HALOE data. *J. Atmos. Sci.* **55**: 163–185.
- Raspollini P, Belotti C, Burgess A, Carli B, Carlotti M, Ceccherini S, Dinelli BM, Dudhia A, Flaud J-M, Funke B, Höpfner M, López-Puertas M, Payne V, Piccolo C, Remedios JJ, Ridolfi M, Spang R, 2006. MIPAS level 2 operational analyses. *Atmos. Chem. Phys. Discuss.* **6**: 5605–5630.
- Rodgers CD, 2000. *Inverse Methods for Atmospheric Sounding: Theory and Practice*. World Scientific Publishing Co.: Singapore.
- Simmons AJ, Hortal M, Kelly G, McNally A, Untch A, Uppala S, 2005. ECMWF analyses and forecasts of stratospheric winter polar vortex breakup: September 2002 in the Southern Hemisphere and related events. *J. Atmos. Sci.* **62**: 668–689.
- Swinbank R, O'Neill A, 1994. A stratosphere–troposphere data assimilation system. *Mon. Weather Rev.* **122**: 686–702.
- Wagner RE, Bowman KP, 2000. Wavebreaking and mixing in the Northern Hemisphere summer stratosphere. *J. Geophys. Res.* **105**: 24799–24808.
- Wargan K, Štajner I, Pawson S, Rood RB, Tan W-W, 2005. Assimilation of ozone data from the Michelson interferometer for passive atmospheric sounding. *Q. J. R. Meteorol. Soc.* **131**: 2713–2734.